Hardware-in-the-Loop Simulation for the Reaction Control System Using PWM-Based Limit Cycle Analysis

Sang W. Jeon and Seul Jung, *Member, IEEE*

***Abstract*—This paper presents numerical studies of analyses of the limit cycle of the reaction control system (RCS) and their validations through hardware-in-the-loop simulation (HILS). The numerical analyses under external disturbance and time-delays of the thruster are confirmed experimentally by HILS for an attitude control system with a single degree of freedom. The thrust of each jet thruster is determined from offline vacuum test results instead of actual thrust measurement. The comparison of HILS results with numerical analysis, shows that predicted properties of the limit cycle is closed to the test results, thus it can be applicable to real RCS. The HILS method allows us to test the RCS without an air-bearing system.**

***Index Terms*—Hardware-in-the-loop simulation (HILS), limit cycle, numerical analysis, reaction control system (RCS), thruster.**

I. Introduction

LIMIT cycle is one of nonlinear characteristics often observed in numerous areas of control systems. Limit cycle phenomena occur when system dynamics has nonlinearities such as friction, actuators with on/off dynamics, and uncertain transport delays [1]–[8]. Limit cycle due to friction [1], [6] and due to on/off dynamics such as braking system or thrusters [5] has been analyzed. The control objective for dealing with limit cycle in the system is to minimize its effects by suppressing amplitudes through prediction methods for adjusting the parameters of the describing functions [2], [3], [6].

In the framework of a launch vehicle, two control systems are generally used for the attitude control of a satellite launch vehicle: the thrust vector control system and the reaction control system. Since a thrust vector control system controls the direction of the engine or nozzles of a launch vehicle, it is effective only when the propulsion system is active. The reaction control system (RCS) controls the thrusters which generate reaction forces by exhausting cold or hot gas through on-off operations of solenoid valves [9], [10].

Many on-off methods for controlling the reaction control system, including bang-bang control, Schmitt trigger control, pulse-width modulator (PWM) control, pulse width frequency modulator control, and derived-rate modulator control are presented [11]. Typically, the PWM control method is used to control electric systems, pneumatic systems, and thruster-controlled spacecraft [12]–[14].

Since the PWM has nonlinear characteristics, such as hysteresis and dead bands, a limit cycle (a periodic behavior appearing as a closed curve in a phase plane) can be observed in the presence of disturbing moments. The properties of the limit cycles can be determined primarily by controller design parameters, level of the thrust, characteristics of the inertia, magnitudes of disturbance, as well as the time delays caused by the opening and closing operation of solenoid valves.

The limit cycle frequency is directly related to the fuel consumption of the system to be controlled. The higher the frequency, the more fuel is required. Thus, it is desirable to analyze the characteristics of the limit cycle to reduce its frequency.

The limit cycle can be analyzed theoretically by using a describing function method [15], [16] and a phase plane method [17]–[21]. The describing function method is an approximate procedure for analyzing nonlinear control. It is based on quasi-linearization which is an approximation of a nonlinear system by a specific family of input waveforms. Generally, the limit cycle can be predicted by the describing function method.

Since the phase plane method indicates the relationship between the velocity and the displacement of a control system in the phase plane, the property of the limit cycle can be obtained. An analysis of the limit cycle in the phase plane method is usually used for thrust selection of jet attitude control systems [17]. Analysis of the limit cycle for integral pulse frequency modulation control has been used in controller design without consideration of control parameters and the time delay effect [20]. Various control methods have been used for attitude control by regulating the on-off states of the thruster [22]–[24].

The limit cycle has been analyzed using the phase plane method, and the corresponding equations have been derived in detail [17], [21]. Haloulakos's method [17], [21] can be applied to a control system, from which the output is described by an on-off state for controlling the thruster. However, his method cannot be used with a PWM control method because the output is described by pulse width [25].

Therefore, unlike the aforementioned methods, the limit cycle analysis in the phase plane method can be used for the traditional proportional derivative (PD) feedback controller design [26]. Input-based PWM control for roll attitude of a launched vehicle is demonstrated through numerical simulation studies.

In this paper, numerical analyses of the frequency, amplitude, duty ratio, and switching line of the limit cycle with control parameters are presented. Those numerical analyses under external disturbances and time-delays of the thruster are confirmed experimentally by HILS for an attitude control system with a single degree-of-freedom.

Manuscript received July 27, 2010; revised January 13, 2011; accepted January 17, 2011. Manuscript received in final form February 14, 2011. Date of publication March 28, 2011; date of current version February 01, 2012. Recommended by Associate Editor M. Lovera.

S. W. Jeon is with Korea Aerospace Research Institute (KARI), Daejeon 305-333, Korea (e-mail: swjeon@kari.re.kr).

S. Jung is with the Mechatronics Engineering Department, Chungnam National University, Daejeon 305-764, Korea (e-mail: jungs@cnu.ac.kr).

Color versions of one or more of the figures in this paper are available online at http://ieeexplore.ieee.org.

Digital Object Identifier 10.1109/TCST.2011.2117427

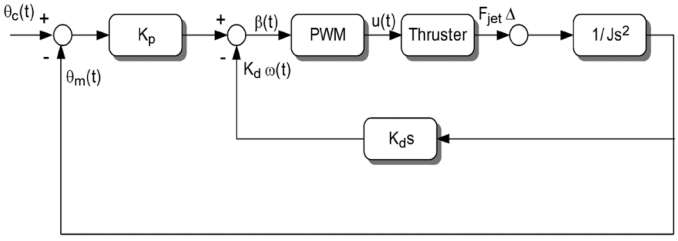

Fig. 1 Roll attitude control system for launch vehicle.

II. Roll Attitude Control System

The attitude of the launch vehicle should be controlled in three mutually perpendicular axes (uncoupled), each with one degree of freedom. The equation of motion for roll direction is given by

$$\frac{d\theta}{dt} = \omega(t) \qquad \frac{d\omega}{dt} = \frac{F_{\text{jet}}\Delta}{J}u(t) \tag{1}$$

$$\omega = \omega_i + \frac{F_{\text{jet}}\Delta}{J}t \tag{2}$$

where θ is the roll angle, ω is the angular velocity, J is the moment of inertia, F_{jet} is the force, Δ is the moment arm, and $u(t)$ is the PWM output.

The block diagram for the PD feedback input-based PWM control system for roll attitude is shown in Fig. 1.

The control command $\beta(t)$ which is a switching line in the phase plane is given when $\theta_c = 0$

$$\beta(t) = -\left(K_p\theta(t) + K_d\omega(t)\right) \tag{3}$$

where K_p is a proportional gain and K_d is a derivative gain. The pulse width of thruster operation is expressed by (4). Equation (4) is determined by the principle of equivalent area given in [14] where t_{ACS} is the sampling time and t_{on} is the control pulse width

$$t_{\text{on}} = \begin{cases} \frac{|\beta(t)|}{F_{\text{jet}}\Delta}t_{\text{ACS}}; & (|\beta(t)| \le F_{\text{jet}}\Delta) \\ \text{sgn}\left(|\beta(t)|\right)t_{\text{ACS}}: & (|\beta(t)| \rangle F_{\text{jet}}\Delta)\,. \end{cases} \tag{4}$$

III. Review of Limit Cycle Analysis

In this section, limit cycle analysis is revisited from [26]. In the case of a roll attitude control system, the main parameters for the controller design are maximum angle, maximum angular rate, frequency of the limit cycle, and duty ratio of the limit cycle. First, magnitudes of the angle and the angular velocity are set at a limit level of the system requirements. The frequency of the limit cycle must be isolated with the natural frequency of system vibration. A low duty ratio is required for a long life span of the thrusters and low gas consumption.

A. Zero External Torque

In this case, the trajectories of the limit cycle are shown in Fig. 2. The problem begins with a set of given initial conditions as described by the angle and angular velocity coordinates at point 1, θ_1 and ω_1 while $t_{\min}$ is the minimum pulse width.

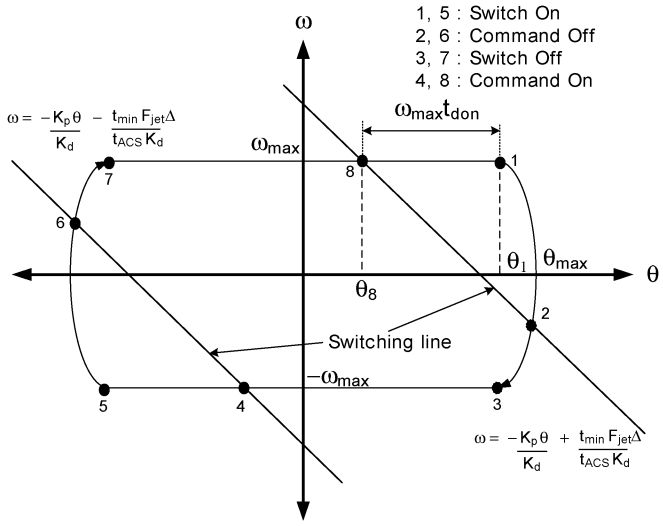

Fig. 2. Limit cycle (zero external torque).

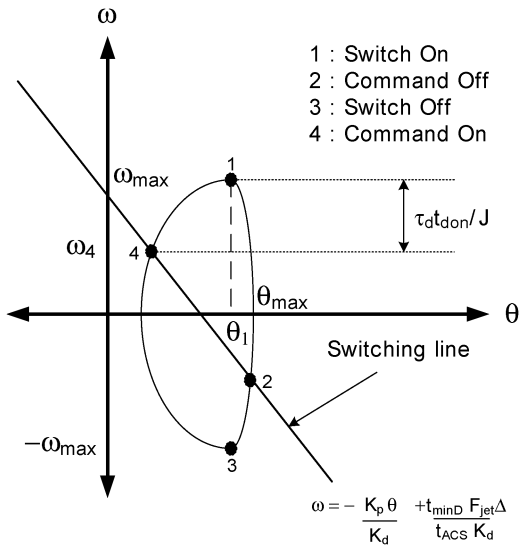

Fig. 3. Limit cycle (constant external torque).

The period T_L, the frequency f, and the duty ratio DR of the limit cycle can be obtained as follows, as found in [26]:

$$T_L = 2t_{\text{on}} + 4\frac{\theta_1}{\omega_{\max}}$$

$$f = \frac{1}{T_L}$$

$$DR = \frac{2(t_{\min} - t_{\text{don}} + t_{\text{doff}})}{T_L} \tag{5}$$

where t_{don} is an on-delay time and t_{doff} is an off-delay time.

B. Constant External Torque

Under a constant external torque τ_d, a reaction jet controller exhibits a limit cycle behavior shown in Fig. 3 (for $\tau_d > 0$, control torque $\tau_c < 0$, and $\tau_c > \tau_d$).

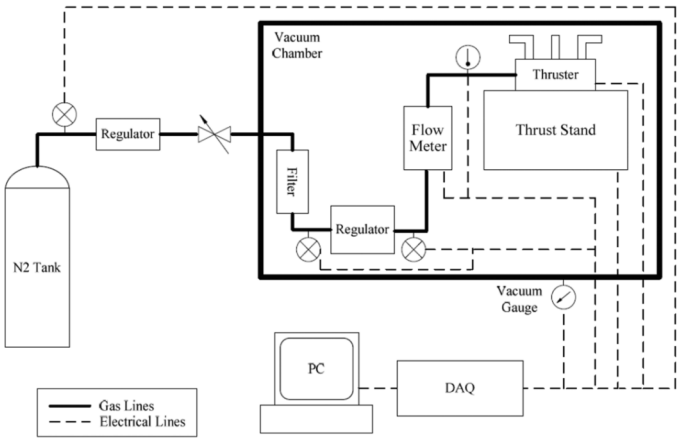

Fig. 4. Schematic diagram of the vacuum thrust measurement system.

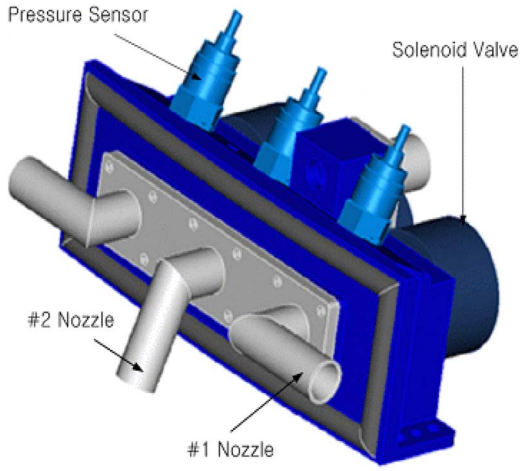

Fig. 5. Configuration of thruster.

The problem also begins with a set of given initial conditions at point 1, θ_1 and ω_1. The frequency and the duty ratio of the limit cycle are given as follows in [26]:

$$T_{LD} = \frac{F_{\text{jet}}\Delta}{\tau_d}(t_{\min} - t_{\text{don}} + t_{\text{doff}})$$
$$f_D = \frac{1}{T_{LD}}$$
$$DR_D = \frac{(t_{\min} - t_{\text{don}} + t_{\text{doff}})}{T_{LD}} \quad (6)$$

where f_D, T_{LD}, and, DR_D are the frequency, the period, and the duty ratio under external torque, respectively.

IV. Thrust Measurement in Vacuum

To perform a precise maneuver, the accurate measurement of the thrust level is essential. Thrust measurement in vacuum is an important factor in designing an accurate attitude controller. In this section, thrust measurement tests are conducted for continuous firing operations.

A. Thrust Measurement System

The thrust measurement system in vacuum is shown in Fig. 4. The system consists of a thruster, two regulators, a thrust stand, a vacuum chamber facility, a flow meter, a data acquisition system, a filter, and a nitrogen gas filling system.

The thruster generates a reaction force by exhausting cold gas through on-off operation of solenoid valves. The thruster consists of a nozzle part for thrust build-up, a solenoid valve part for on-off valve operations, a body part for gas flow and connections with other parts. The configuration of the thruster for Korea Space Launch Vehicle-I (KSLV-I) is shown in Fig. 5.

The thrust stand is an inverted pendulum type with short thin stainless steel plates at four corners to act as load springs for the thrust force as well as to support the weight of the thruster assembly. The natural frequency of the thrust stand system including the thruster and gas tube between the flow meter and the thruster is approximately 100 Hz. The natural frequency of the thrust stand system is dictated by the gas tubing between the flow meter and the thruster. The tubing is much stiffer than the four thin plates.

Experiments are conducted in a vacuum chamber 1 m long and 1 m diameter at Korea Aerospace Research Institute (KARI). The vacuum chamber is pumped by two large rotary pumps, each of which has a maximum pumping speed of 7200 L/min. The pumping path has a diameter of approximately 0.1 m and a length of approximately 3 m. The conductance of the pumping path is roughly 1 100 000 L/m in for viscous flow. The ambient vacuum pressure is kept below 100 Torr (in most cases, below 50 Torr) in all tests.

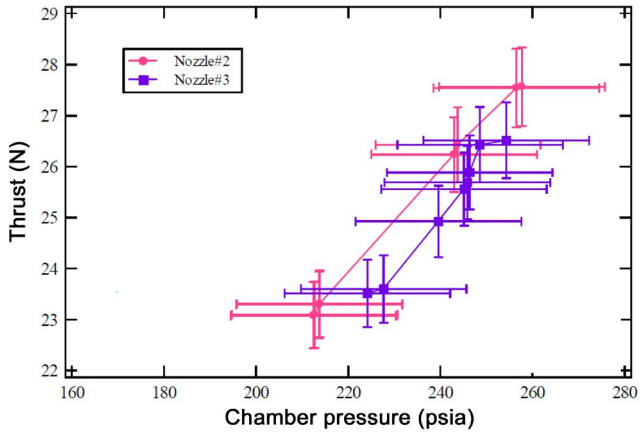

Fig. 6. Thrust at ambient vacuum pressure.

B. Measurement Tests

Thrust measurement tests are conducted for continuous firing operations. There are 3 firings for each of which the time is 6 s, off time is 2 s, duty ratio is 75%, and frequency is 0.125 Hz.

The purpose of continuous firing tests is to collect thrust data that show basic thruster performance in vacuum condition used for calculations of total impulses of pulse firing tests. In addition to the basic thruster performance, the collected data are analyzed for the dependence of thrust on thruster chamber pressure and ambient vacuum pressure. The continuous firing tests are also conducted to compare the performance of different nozzles.

The measurement results for thrust at ambient vacuum pressure are summarized in Fig. 6. The data from the thrust measurement tests such as thrust, pressure, and temperature are subject to errors associated with the uncertainty in the measurement system and sensors. It is clear that the thruster produces thrusts

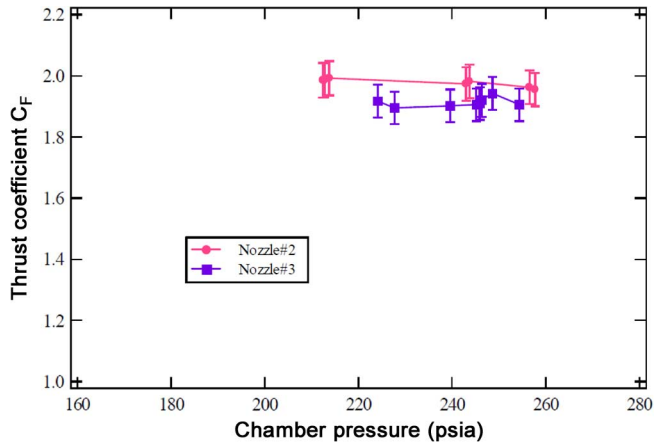

Fig. 7. Thrust coefficient at ambient vacuum pressure.

between 23 to 28 N ($+/-0.8$ N: error band). A general trend of increasing thrust with an increasing chamber pressure can be seen in Fig. 6.

The thrust equation is described as

$$F_{th} = \int PdA = A_t P_c C_F \tag{7}$$

where F_{th} is the thrust, A_t is the throat area, P_c is the chamber pressure of thruster, and C_F is the thrust coefficient [27].

Fig. 7 illustrates the difference between two nozzles by comparing their thrust coefficients. The thrust coefficient determines the amplification of the thrust due to the gas expansion in the nozzle as compared to the thrust that would be exerted if the chamber pressure acts over the throat area only.

V. HILS

The thruster vector control system is used for pitch and yaw attitude control and the RCS is used for roll attitude control during the thrusting phase. In this section HILS is presented for a roll control system of the upper stage of the KSLV-I, capable of injecting a 100 kg class satellite into a low earth orbit.

A. Hardware

The RCS which consists of pneumatic and control parts is to be installed on the KSLV-I upper stage. The pneumatic part consists of the bottle part for storing nitrogen gas, the valve part for flow control of the nitrogen gas, the thruster part for thrust generation, the tube part for connecting all the pneumatic components, and the propellant part. The control part consists of a thruster control unit (TCU) which controls the valves and monitors the system, and electrical cables. The schematic diagram of the pneumatic part for the RCS is shown in Fig. 8.

To verify the analysis results of the limit cycle, a HILS with the RCS for KSLV-I was performed using the chamber pressures of the thrusters. The chamber pressure and thrust in vacuum are in the proportions as shown in Fig. 6. The measured chamber pressures are converted into thrusts by a HILS computer. The attitude of the launch vehicle is changed by the flight dynamics, and then the inertia navigation and guidance unit (INGU) module in the HILS computer generates a new attitude control command. Then the TCU controls the solenoid valves

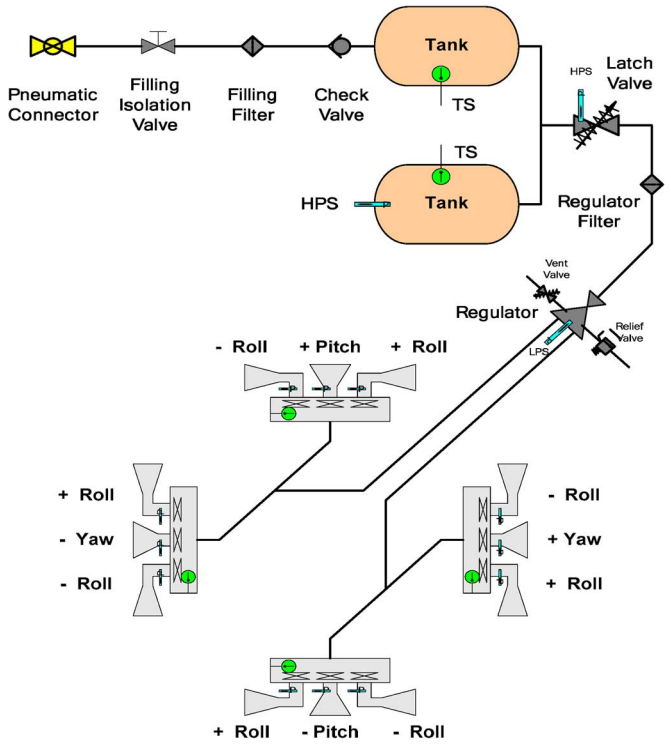

Fig. 8. Schematic diagram of the pneumatic part for the RCS.

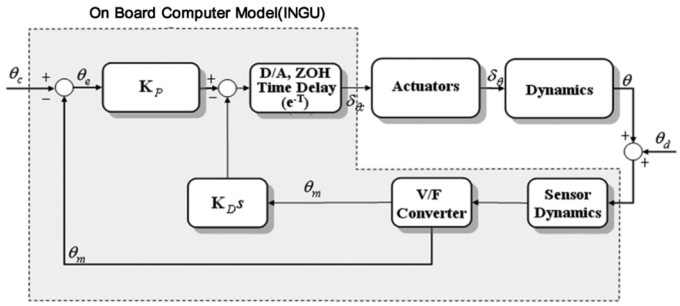

Fig. 9. INGU software model.

of the RCS. The thruster chamber pressures are varied by the operation of the TCU. In this way, the closed loop is repeated.

The INGU is implemented with linearized equations (sensor dynamics, time delay, and converter model). The INGU software model is shown in Fig. 9.

The hardware of the HILS consists of the RCS, TCU, a MATLAB host computer, a MATLAB Real-Time-Workshop HILS computer including an INGU model, a control console for the TCU, and a test box for the TCU and two I/O boxes. The block diagram of the HILS is shown in Fig. 10.

The HILS of KSLV-I was carried out for the whole RCS control loop. Flight dynamics models with one degree-of-freedom and the INGU models are coded into a real-time simulation program and embedded into a real-time computer. The analog/digital interface is set up for the RCS chamber pressure measurements. A digital IO is also set up for the communication of thruster on/off commands and control enable signals. Fig. 11 shows a photograph of the hardware setup of the HILS. The parameters are listed in Table I.

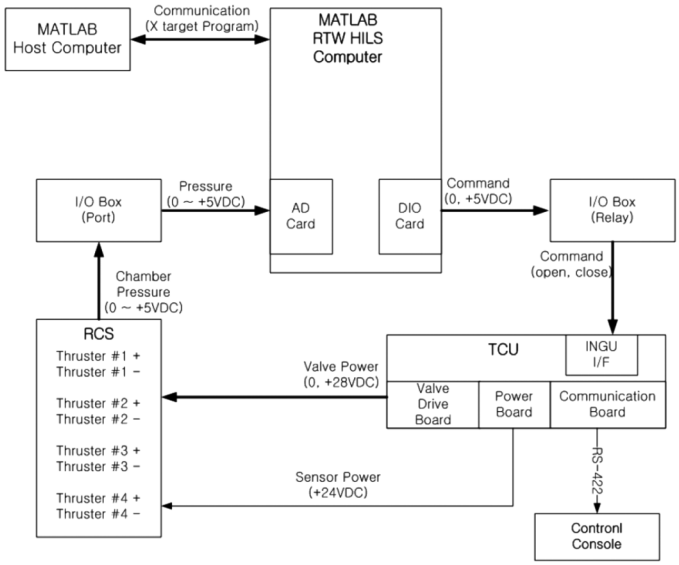

Fig. 10. Block diagram of HILS.

Fig. 11. Operational setup of HILS.

B. HILS Results

1) Zero External Torque: First, no external torque is applied. The corresponding HILS results are shown in Figs. 12–15. Fig. 12 shows the calculated control thrust by the chamber pressure. It is about 92 N for the positive attitude control or about 86 N for the negative attitude control. Fig. 13 shows the on-delay time (t_{don}), off-delay time (t_{doff}), and an overshoot phenomenon. The on-delay time is about 13 ms and the off-delay time is about 20 ms. We observed overshoot responses for every thruster activations. Fig. 13 shows that the thrust is 7% higher during 15 ms after the valve is open.

Fig. 14 shows the roll attitude trajectory in the phase plane. Fig. 15 shows the larger image of the limit cycle portion of Fig. 14. The value of point 1 in Fig. 15 is changed with time because of the difference between the positive and negative control

TABLE I
SIMULATION PARAMETERS

Parameter	Value
Flight time	72.2 s
Moment of inertia	501 kgm^2
Moment arm	1 m
Sampling time	0.3 s
Proportional gain	987.6
Derivative gain	1094.9
Constant external torque	0 N or 44 N
Initial angle error	10 $deg.$
Integration time step	0.001 s

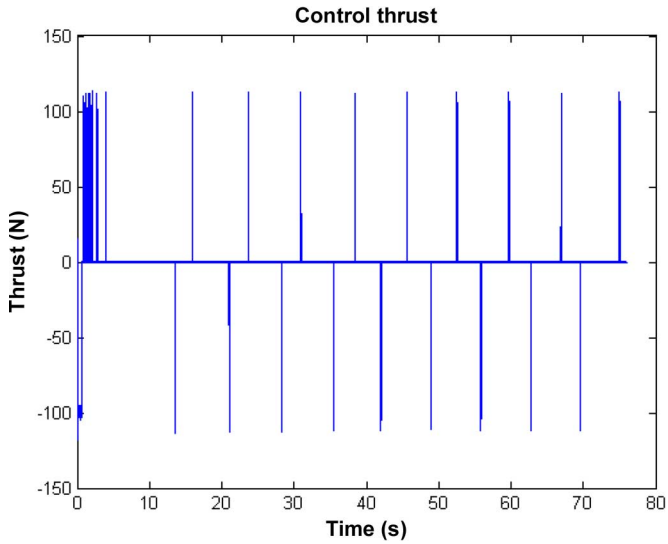

Fig. 12. Control thrust (zero external torque is applied).

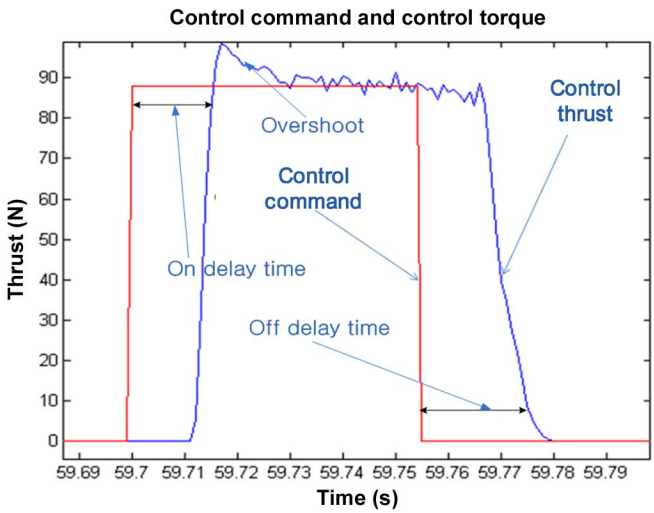

Fig. 13. Delay times and overshoot phenomenon.

Fig. 14 shows the roll attitude trajectory in the phase plane. Fig. 15 shows the larger image of the limit cycle portion of Fig. 14. The value of point 1 in Fig. 15 is changed with time because of the difference between the positive and negative control

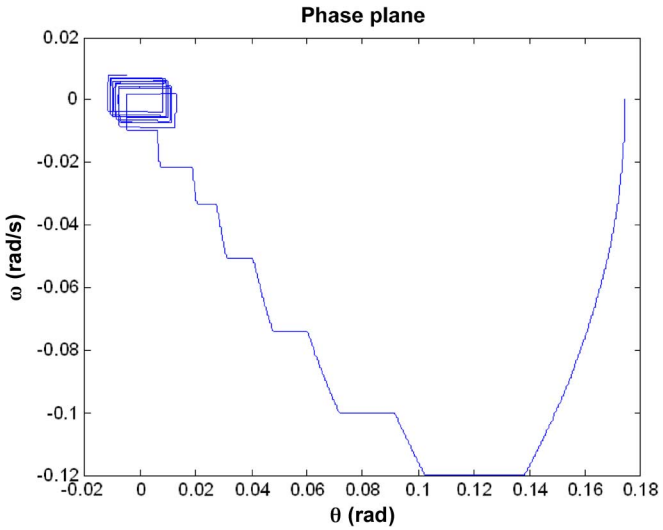

Fig. 14. Trajectory in the phase plane (zero external torque).

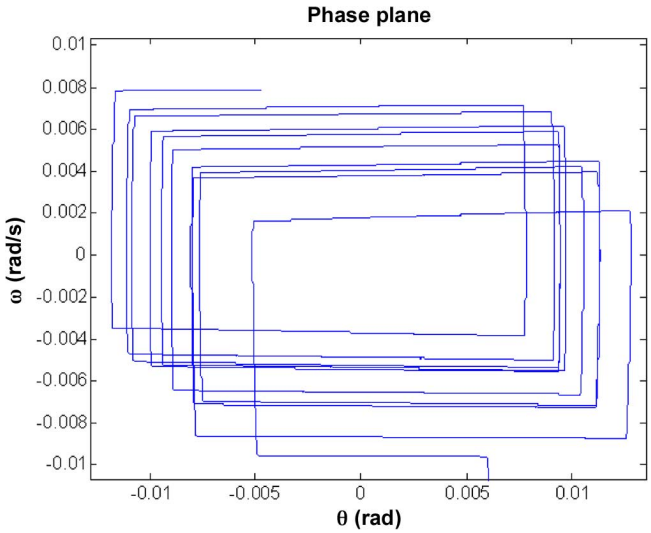

Fig. 15. Limit cycle trajectory (zero external torque is applied).

torque levels, on-off delay time, and the overshoot phenomenon in the real hardware system.

The frequency of the limit cycle, 0.108 Hz and the duty ratio, 1.3% are obtained by using simulation parameters and thrust level defined in (5). The frequency of the limit cycle and the duty ratio obtained by the HILS results are 0.145 Hz and 1.94%. There is about 20% and 40% errors between calculation and HILS because of the positive and negative control torque level, the overshoot phenomenon, and the time varying on-off delay time in the real system. However, in the case of errorless system, the frequency of limit cycle and duty ratio is quite close as in [26].

2) Constant External Torque: The second experiment is performed when a constant external torque is applied. Fig. 16 shows the calculated control thrust by the chamber pressure. The range varies from 95 to 78 N. Fig. 17 shows the roll attitude trajectory in the phase plane. Fig. 18 shows the larger image of the limit cycle portion of Fig. 17. We observe quite a different behavior in Fig. 18 comparing with Fig. 15. The value of point 1 changes with time because the thrust level in Fig. 16 is time-varying.

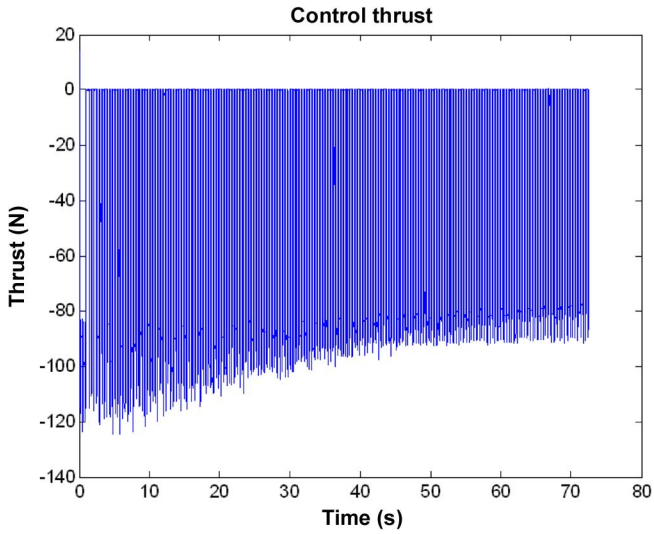

Fig. 16. Control thrust (constant external torque is applied).

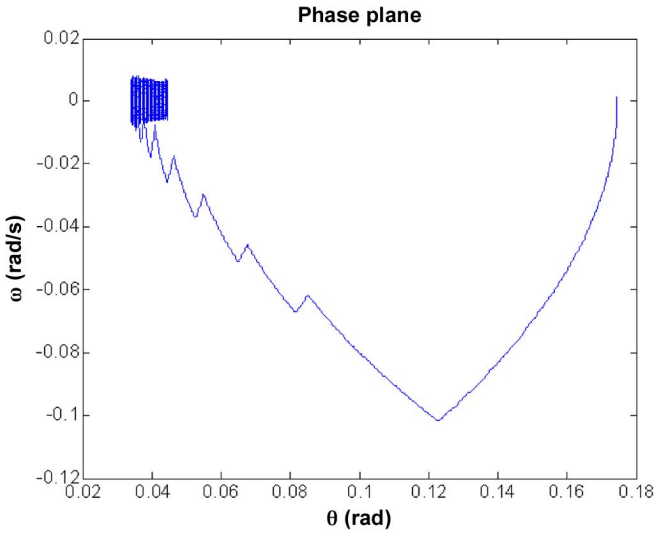

Fig. 17. Trajectory in the phase plane (constant external torque is applied).

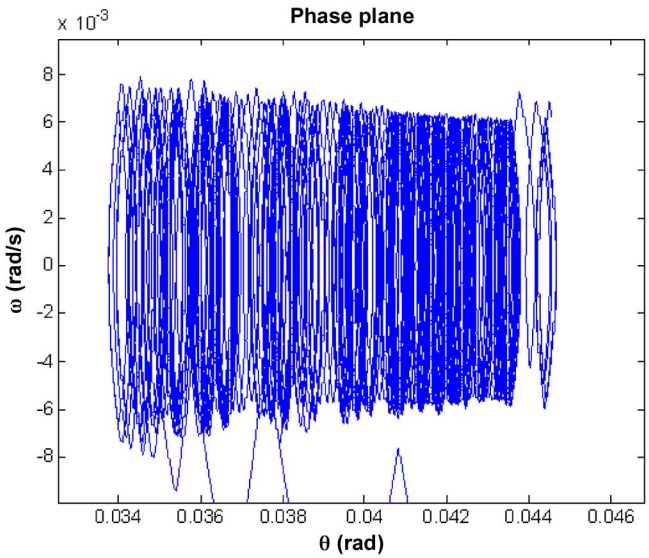

Fig. 18. Limit cycle trajectory (constant external torque is applied).

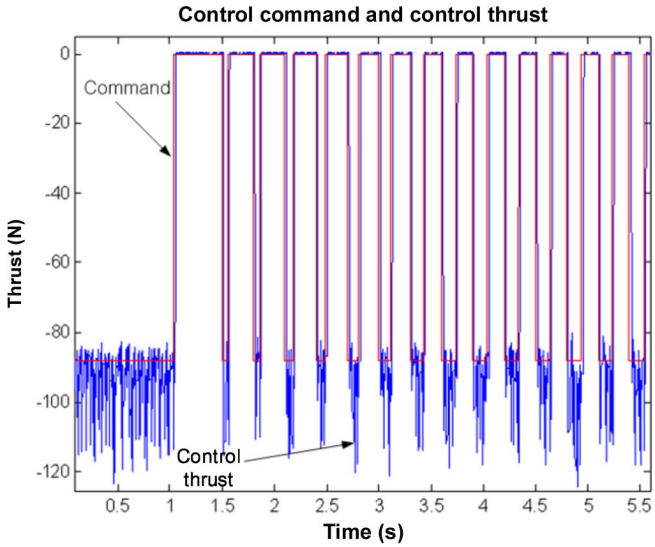

Fig. 19. Control thrust and command (initial).

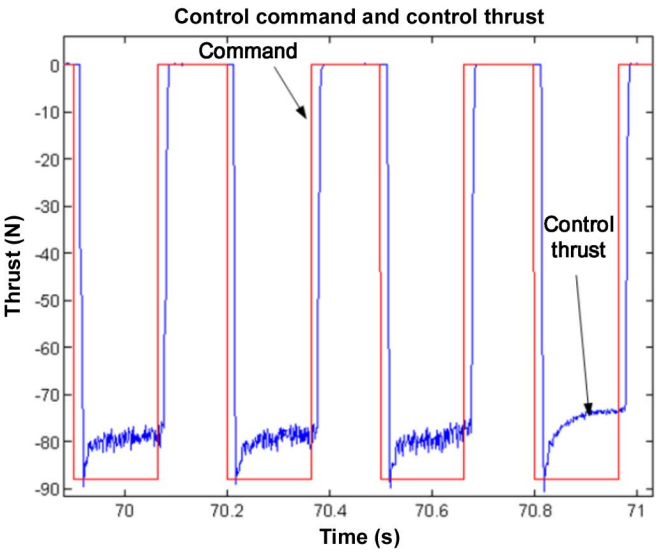

Fig. 20. Control thrust and command (final).

This behavior happens when the regulator in Fig. 8 changes the tank pressure. If the tank pressure is dropped under a fixed pressure, the regulated pressure is also dropped. Figs. 19 and 20 are larger images of an initial part and a final part of Fig. 16, respectively.

The regulated pressure varies with time from 240 to 182 psia. Under normal operating conditions, the regulated pressure is varied from 220 psia ($+/-20$ psia). However, in case of the finial condition in Fig. 20, the regulated pressure is falling as the tank pressure changes. The tank pressure is dropped by the operation of thruster.

The calculated frequency of the limit cycle and the duty ratio defined in (6) are 3.333 Hz and $46.3 \sim 56.4\%$ by analysis. The frequency of limit cycle and the duty ratio by HILS are 3.333 Hz and $49.1 \sim 58.2\%$. Although the control torque is time-varying, simulation results are quite close to the HILS results. This consolidates that the limit cycle analysis corresponds to the limit cycle of the real system. Therefore, the attitude control parameters using the proposed limit cycle analysis can be easily designed.

VI. Conclusion

In this paper, experimental studies of the limit cycle for the attitude control system in jet thrusters using the chamber pressure of the thruster are presented. HILS is applied to the RCS of KSLV-I using the chamber pressures of the thrusters. The thrust is determined from off-line vacuum test results instead of actual thrust measurement. The comparison of HILS results with numerical analysis, shows that predicted properties of the limit cycle is closed to the test results, thus it can be applicable to real RCS. The HILS method allows us to test the thruster without an air-bearing system, which has a difficulty in the balance.

References

[1] H. Olsson and K. J. Astron, "Friction generated limit cycles," *IEEE Trans. Control Syst. Technol.*, vol. 9, no. 4, pp. 629–636, Jul. 2001.
[2] B. F. Wu and J. W. Perng, "Limit cycle analysis of PID controller design," in *Proc. Amer. Control Conf.*, 2003, pp. 2424–2429.
[3] J. W. Perng, B. F. Wu, H. I. Chin, and T. T. Lee, "Limit cycle analysis of uncertain fuzzy vehicle control systems," in *Proc. IEEE Conf. Netw., Sens. Control*, 2005, pp. 626–631.
[4] Y. J. Wang, "Robust limit cycle amplitude suppression for a class of uncertain nonlinear control systems," in *Proc. ICARCV*, 2006, pp. 1–6.
[5] M. Tanelli, G. Osorio, M. D. Bernardo, S. M. Savaresi, and A. Astolfi, "Limit cycles analysis in hybrid anti-lock braking systems," in *Proc. IEEE Conf. Dec. Control*, 2007, pp. 3865–3870.
[6] Y. J. Huang and Y. J. Wang, "Limit cycle analysis of electro-hydraulic control systems with friction and transport delay," in *Proc. World Congr. Intell. Control Autom.*, 2000, pp. 3306–3311.
[7] E. G. Papadopoulos and G. C. Chasparis, "Analysis and model-based control of servomechanisms with friction," in *Proc. IROS*, 2002, pp. 2109–2114.
[8] S. T. Impram and N. Munro, "Limit cyle analysis of uncertain control systems with multiple nonlinearities," in *Proc. IEEE Conf. Dec. Control*, 2001, pp. 3423–3428.
[9] G. R. Cho, "Research and development of KSLV-I(V)," MOST, Daejeon, Korea, 2007.
[10] S. Adler, A. Warshavsky, and A. Peretz, "Low-cost cold-gas reaction control system for slohsat FLEVO small satellite," *J. Spacecraft Rocket*, vol. 42, no. 2, pp. 345–351, Mar.–Apr. 2005.
[11] B. Wie, "Spacecraft dynamics and control: Application of dynamical systems theory," Arizona State Univ., Tempe, 1995.
[12] L. M. Tolbert, F. X. Peng, and T. G. Habetler, "Multilevel PWM methods at low modulation indices," *IEEE Trans. Power Electron.*, vol. 15, no. 4, pp. 719–725, Jul. 2000.
[13] X. Shen, J. L. Zhang, E. J. Barth, and M. Goldfarb, "Nonlinear model-base control of pulse width modulated pneumatic servo system," *ASME J. Dyn. Syst., Meas., Control*, vol. 128, pp. 663–669, 2006.
[14] T. Ieko, Y. Ochi, K. Kanai, N. Hori, and P. N. Nikiforuk, "Design of a pulse-width-modulation spacecraft attitude control system via digital redesign," in *Proc. IFAC 14th Triennial World Congr.*, 1999, pp. 355–360.
[15] B. F. Wu, J. W. Perng, and J. I. Chin, "Limit cycle analysis of nonlinear sampled-data systems by gain-phase margin approach," *J. Franklin Inst.*, vol. 342, pp. 175–192, 2005.
[16] C. C. Cheng and C. H. Huang, "On the limit cycle of the underwater vehicle control system," in *Proc. Int. Symp. Underwater Technol.*, 1998, pp. 461–465.
[17] V. E. Haloulakos, "Thrust and impulse requirements for jet attitude-control systems," *J. Spacecraft*, pp. 84–90, 1964.
[18] M. H. Kaplan, *Modern Spacecraft Dynamics and Control*. New York: Wiley, 1976, p. 261.

[19] S. J. Dodds, "A predicted signed switching time high precision satellite attitude control law," *Int. J. Control*, pp. 1051–1061, 1984.

[20] H. B. Hablani, "Target acquisition, tracking, spacecraft attitude control, and vibration suppression with IPFM reaction jet controllers," in *Proc. AIAA Guid., Nav. Control Conf.*, 1992, pp. 1118–1137.

[21] V. E. Haloulakos, "Analysis of jet attitude control systems subject to varying magnitudes of external disturbing torques," in *Proc. AIAA, Guid., Control Flight Dyn. Conf.*, 1967, pp. 1–11.

[22] W. E. Vander Velde, "Design of space structure control systems using on-off thrusters," *J. Guid.*, vol. 6, pp. 53–60, 1983.

[23] E. F. Breitfeller and L. C. Ng, "A nonlinear fuel optimal reaction jet control law," presented at the 11th AIAA/MDA Technol. Conf. Exhibit, Monterey, CA, 2002, paper no. 6-5.

[24] W. C. Stone, "Fast variable-amplitude cold gas thruster," *J. Spacecraft Rockets*, vol. 32, no. 2, pp. 335–343, 1995.

[25] F. Bernelli-Zazzera, P. Mantegazza, and V. Nurzia, "Multi-pulse-width modulated control of linear system," *J. Guid.*, vol. 21, pp. 64–70, 1998.

[26] S. W. Jeon and S. Jung, "Novel analysis of limit cycle for PWM signal of PD control system," *IEICE Electron. Expr.*, vol. 6, no. 11, pp. 787–793, 2009.

[27] R. W. Humble, G. N. Henry, and W. J. Larson, *Space Propulsion Analysis and Design*. New York: McGraw-Hill, 1995.